

Whiteness metric for light sources of arbitrary color temperatures: proposal and application to light-emitting-diodes.

Aurelien David,^{1,*} Michael R. Krames¹ and Kevin W. Houser²

¹ Soraa Inc., 6500 Kaiser Drive, Fremont, CA 94555, USA

² Department of Architectural Engineering, The Pennsylvania State University, University Park, PA 16802, USA

[*adavid@soraa.com](mailto:adavid@soraa.com)

Abstract: We study the quantification of whiteness perception under illumination from various light sources. We discuss an existing metric for sources with high correlated color temperature (CCT), CIE whiteness, and propose a procedure to adapt it to sources of any CCT. We illustrate our approach by comparing the ability of different warm-white sources to render whiteness. We show that a careful engineering of the spectrum – facilitated by the flexibility of light-emitting diode sources – is essential to render whiteness.

© 2013 Optical Society of America

OCIS codes: (330.1715) Color, rendering and metamerism; (230.3670) Light-emitting diodes

References and links

1. E. Ganz, “Whiteness - photometric specification and colorimetric evaluation,” *Appl. Opt.* **15**(9), 2039–2058 (1976).
2. P. S. Stensby, “Questions in regard to whiteness evaluation,” *Journal of Color Appearance* **2**(1), 39–42 (1973).
3. D. L. MacAdam, “Specification of whiteness,” *J. Opt. Soc. Am.* **24**(7), 188 (1934).
4. R. S. Hunter, “Description and measurement of white surfaces,” *J. Opt. Soc. Am.* **48**(9), 597–605 (1958).
5. F. Grum, R. F. Witzel, and P. Stensby, “Evaluation of whiteness,” *J. Opt. Soc. Am.* **64**(2), 210–215 (1974).
6. E. Ganz, “Whiteness formulas - a selection,” *Appl. Opt.* **18**(7), 1073–1078 (1979).
7. E. Ganz, “Whiteness perception - individual-differences and common trends,” *Appl. Opt.* **18**(17), 2963–2970 (1979).
8. P. Kraus, “On a new black and a new white,” *Melliand Textileber* **10**, 468 (1929).
9. A. E. Siegrlst, H. Hefti, H. R. Meyer, and E. Schmidt, “Fluorescent whitening agents 1973-1985,” *Review of Progress in Coloration and Related Topics* **17**(1), 39–55 (1987).
10. J. Schanda (Editor), *Colorimetry: Understanding the CIE System* (John Wiley and Sons, Hoboken (NY), 2007).
11. J. C. Zwinkels and M. Noel, “CIE whiteness assessment of papers: impact of LED illumination,” in “27th Session of the CIE,” (Sun City, South Africa, 2011).
12. “Colorimetry, 3rd edition,” CIE Technical report **CIE 15.3:2004** (2004).
13. B. D. Jordan and M. A. O’Neill, “The whiteness of paper - colorimetry and visual ranking,” *TAPPI Journal* **74**(5), 93–101 (1991).
14. “Paper and board - determination of CIE whiteness, D65/10° (outdoor daylight),” ISO norm **11475:2004(E)** (2004).
15. “Paper and board - determination of CIE whiteness, C/2° (indoor illumination conditions),” ISO norm **11476:2010(E)** (2010).
16. R. Griesser, “Assessment of whiteness and tint of fluorescent substrates with good interinstrument correlation,” *Col. Res. Appl.* **19**(6), 446–460 (1994).
17. R. Griesser, “CIE whiteness and tint : possible improvements,” *APPITA Journal* **49**(2), 105 (1996).
18. E. Ganz and R. Griesser, “Whiteness - assessment of tint,” *Appl. Opt.* **20**(8), 1395–1396 (1981).

19. H. Hemmendinger and J. Lambert, "The importance of chromaticity in the evaluation of whiteness," *Journal of the American Oil Chemists Society* **30**(4), 163–168 (1953).
20. I. Katayama, K. Masumi, and T. Aoki, "Quantitative evaluation of perceived whiteness under different illuminations," *Journal of Light and Visual Environment* **31**(2), 80–88 (2007).
21. M. Ayama, T. Akatsu, E. Toriumi, K. Mukai, and S. Kanaya, "Whiteness perception under different types of fluorescent lamps," *Col. Res. Appl.* **28**(2), 96–102 (2003).
22. I. Katayama, M. Iiyama, and K. Masumi, "Effect of spectral distribution of an illuminant on perceived whiteness," *Journal of Light and Visual Environment* **25**(2), 41 (2001).
23. Indeed, ω represents the relative sensitivity of luminance factor Y and blue-shift to whiteness. In our samples the value of Y barely depends on the source, only the color shift is significantly different. Therefore a change in ω would rescale the whiteness values but would not change the relative rankings of whiteness under the different sources. Regarding ϕ , its value has a very small numerical effect so long as it is close to 0° , as discussed in [1].
24. M. J. Cich, R. I. Aldaz, A. Chakraborty, A. David, M. J. Grundmann, A. Tyagi, M. Zhang, F. M. Steranka, and M. R. Krames, "Bulk GaN based violet light-emitting diodes with high efficiency at very high current density," *Appl. Phys. Lett.* **101**(22), 223509 (2012).
25. J. Zwinkels, "Surface fluorescence: the only standardized method of measuring luminescence," in "Standardization and Quality Assurance in Fluorescence Measurements I," vol. 5 of *Springer Series on Fluorescence, U. Resch-Genger Editor* (Springer Berlin Heidelberg, 2008), pp. 163–192.
26. "Calibration methods and photoluminescent standards for total radiance factor measurements," CIE Technical report **CIE 182:2007** (2007).

1. Whiteness enhancement

Whiteness perception is an important part of our visual experience. Together with color rendering, white rendering determines how natural and pleasant object rendition is. The perception of whiteness is a complex sensorial effect. One might expect that a perfect white diffuser with reflectivity $R=1$ at all wavelengths (a reference white) would be perceived as the whitest possible surface. However, it has long been known that brightness and tint can substantially modify whiteness perception. Several perceptual studies have established the following trends [1–7]:

- total luminance contributes to whiteness (e.g. if two objects have the same color coordinates (x, y) , the brighter object will appear whiter)
- objects with a slight blue saturation (toward the dominant wavelength $\lambda_d = 470$ nm) are perceived as whiter than the reference white, while objects with a yellow saturation (away from $\lambda_d = 470$ nm) appear less white. Excessive blue saturation diminishes whiteness perception.
- objects with an excessive red or green tint (e.g. with color shifts perpendicular to the saturation direction $\lambda_d = 470$ nm) do not appear white.

Therefore, an object can be made to appear whiter than the reference white by having high overall reflectance and a slight blue saturation. Early on, this was harnessed by dyeing objects to reduce their yellow reflectance and induce a slight color shift [3]. As early as 1929 [8], the use of fluorescent whitening agents [9] (FWAs) was observed to provide a strong enhancement of whiteness in textiles. FWAs are substances which absorb ultra-violet (UV, $\lambda < 380$ nm) radiation and violet (V, $380 < \lambda < 420$ nm) light, and re-emit blue-cyan light. By adding FWAs to a material in addition to yellow-absorbing dyes, the color shift can become substantial: if the source has significant ultra-violet and violet (UV/V) content, strong blue fluorescence is induced, yielding a strong impression of whiteness.

Over the decades the use of FWAs has become commonplace in white materials including plastics, paper, fiber, textiles, detergent and cosmetics [10]; manufacturers spend considerable efforts to assess and increase the whiteness of their products. On the other hand, the potential of a light source to improve whiteness perception is rarely considered. Whiteness, however, is not only a material property; it is dependent upon the interaction between a material and its illumination. Daylight has significant UV/V content, leading to a very pronounced whiteness enhancement in the presence of FWAs. Incandescent warm-white sources contain less UV/V, and will induce a moderate whiteness enhancement. Most existing light-emitting diodes (LEDs) have little to no UV/V content, and thus offer limited prospects for whiteness enhancement – a

shortcoming discussed in [11]. However, as will be shown in this article, the spectrum of LEDs can be purposely tailored to affect whiteness perception.

In this article, we discuss the perception of whiteness for various sources. We review CIE whiteness (a recognized metric to quantify whiteness perception) and propose an approach to generalize this metric to sources of varying correlated color temperature (CCT). We show, in particular, how our modified metric can be used to assess the ability of warm-white sources to render whiteness. We discuss how the source's spectrum can be tailored to enhance whiteness, an approach that is especially relevant to LEDs.

2. CIE whiteness – definition and generalization to other CCTs

2.1. CIE whiteness formula

There has been significant effort to quantify whiteness on a numerical scale. Many formulas have been developed over the years [1, 4–7]. Among these, the formula proposed by the Commission Internationale de l'Éclairage (CIE) [12] presents several advantages: it usually shows good correlation to perceptual studies (within its application range) [13]; it is easy to compute; and it is the object of two international norms (ISO 11475 – 2004 and 11476 – 2010 for outdoors and indoors illumination, respectively [14, 15]).

The basis of the CIE whiteness formula is to consider the color shift of an object from a reference illuminant. Whiteness and tint are affected by this shift. The general linear form of such an equation is [16, 17]:

$$W = Y - \omega \cdot \cos(\eta + \varphi) / \cos(\varphi) \cdot (x - x_0) - \omega \cdot \sin(\eta + \varphi) / \cos(\varphi) \cdot (y - y_0) \quad (1)$$

Y is the Y -tristimulus value of the sample, i.e. its luminance factor (a perfect reflector has $Y = 100$); ω is the sensitivity of whiteness to saturation (e.g. to a color shift along λ_d); η is the angle between the x -axis and the direction of λ_d , i.e. $\tan(\eta) = (y_0 - y_d) / (x_0 - x_d)$; φ is a small angle which represents tint preference (e.g., the fact that maximal whiteness enhancement is not exactly in the direction of λ_d); (x_0, y_0) are the coordinates of the reference illuminant; (x_d, y_d) are the coordinates the dominant wavelength; and (x, y) are the coordinates of the object under consideration. All these quantities pertain to a specific color space and the corresponding color-matching functions (CMFs). The values of ω and φ are derived from experimental data [6].

In practice, the following values are used for the definition of CIE outdoors whiteness [6] (which employs reference illuminant D65 and the CIE 1964 10° standard observer [12]): $\omega = 1800$, $\varphi = 16.6^\circ$, $(x_0, y_0) = (0.3138, 0.3310)$, $(x_d, y_d) = (0.1152, 0.1090)$, $\eta = 48.2^\circ$. This results in the numerical formula of CIE whiteness [14]:

$$W = Y + 800(x_0 - x) + 1700(y_0 - y) \quad (2)$$

These values pertain to the so-called outdoors whiteness standard. Another ISO standard was also later defined for so-called indoors whiteness, employing the CIE 1931 2° standard observer and illuminant C, resulting in slightly different numerical values of ω , φ and η [15]. Outdoors whiteness is more sensitive to the presence of FWAs, while indoors whiteness is more representative of common conditions such as office environments.

The value of the coefficients in Eq. (2) is worthy of a few comments. The unity coefficient before Y sets an absolute scale for whiteness: for a sample with no tint ($x = x_0$, $y = y_0$), i.e. a perfect gray, whiteness is equal to Y . Therefore, a sample with a spectrally flat reflectance of 90% has a whiteness of 90. A luminance difference of 10% is rather easily detected visually, indicating that a 10-point change in whiteness is significant. For tinted samples, the value of ω was chosen by determining what color shift was perceived as equivalent to a given change in Y ;

thus a shift in color coordinates of about 0.005 (in the direction of λ_d) is perceived as similar to a 10-points increase in reflectance.

Equation (2) favors certain color shifts; however these should not be in a direction inducing excessive tint as the sample would no longer look white. Sample tint is further defined as [18]:

$$T = -\zeta \cdot \sin(\eta') \cdot (x - x_0) + \zeta \cdot \cos(\eta') \cdot (y - y_0) \quad (3)$$

In principle, $\eta' \sim \eta$ (tint occurs for color shifts perpendicular to λ_d). In practice both η' and ζ were obtained from fitting experimental data, yielding $\eta' = 54^\circ$, $\zeta = 1110$ and:

$$T = 900(x_0 - x) - 650(y_0 - y) \quad (4)$$

Again, these values pertain to outdoors illumination and employ the 10° standard observer. A similar equation, with slightly different coefficients, stands for indoors illumination under the 2° standard observer.

Figure 1 clarifies the geometry involved in the definition of CIE whiteness. The main direction is along the axis defined by the chromaticity of the illuminant and the spectrum locus at a dominant wavelength $\lambda_d = 470$ nm. Shifts (nearly) parallel to this direction (with a small angle ϕ) correspond to whiteness. Shifts (nearly) perpendicular to this direction correspond to tint.

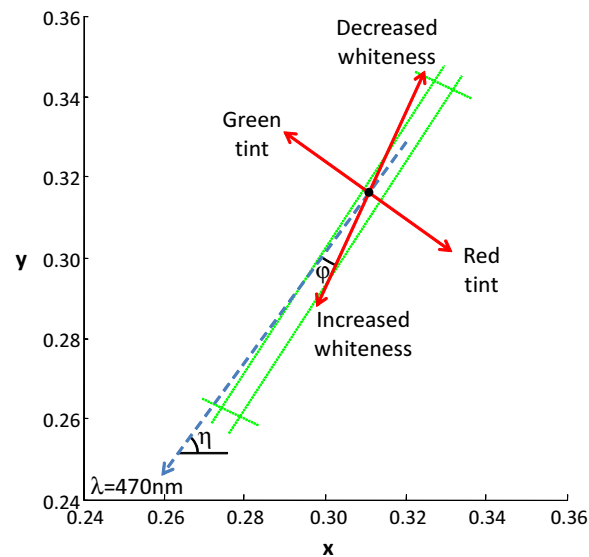


Fig. 1. Geometry corresponding to the CIE whiteness formula. The black dot is the white point of the reference illuminant. Tint variations are nearly perpendicular to the dominant wavelength; whiteness variations are nearly parallel to it (the small angle ϕ accounts for average tint preference). The dotted box illustrates the limits of the CIE formula (upper and lower bounds for whiteness and tint).

Equation (2) was designed for a relative comparison of different objects illuminated by D65. In the practical application of Eq. (2), experimental measurements of whiteness are frequently performed in colorimeters/spectrophotometers whose light source is not D65 (although it attempts to approximate it in the visible range). Depending whether the light source has more or less UV/V content than D65, the measured value of whiteness is larger or smaller than it would be under D65. This effect is usually seen as a metrology problem in the accurate determination

of whiteness [16]. However, it also corresponds to a perceptual reality: the perceived whiteness of an object containing FWAs strongly depends on the source's UV/V spectrum, a worry noted early in [19]. For instance, the perceived whiteness of a white paper under a 6500 K fluorescence lamp is much lower than under D65 or daylight due to the lower UV/V output.

Therefore, although Eq. (2) was designed to characterize relative whiteness of two or more samples under a fixed reference illuminant, it could also be employed to characterize the relative potential of several light sources to render whiteness for a fixed reference object – provided that the sources have the same color coordinates (x_0, y_0) (and hence the same CCT) as D65. By comparing the resulting whiteness values, one can predict the relative perceived whiteness of the object under these sources.

2.2. Perception of whiteness vs. CCT

As previously mentioned, Eq. (2) was derived following a series of human perception experiments. The sources used during these studies were either daylight or artificial sources aiming to replicate D65, hence the choice of the reference illuminant for Eq. (2). One may wonder if the ingredients for perceived whiteness (namely, a shift towards a dominant wavelength of 470 nm and no pronounced red or green hue) can be generalized to other CCTs, especially since chromatic adaptation will adjust an observer's whiteness perception.

In a study [20], participants were shown a series of Munsell chips close to a neutral white, but with slight tints in various directions of the color space; they were asked to rank the chips for whiteness. The study was performed under a variety of CCTs between 3000 K and 6500 K. Participants systematically ranked blue/purple chips as whiter than a neutral white, and yellow/red chips as less white; the quantitative rankings were similar under all CCTs for all the chips. This suggests that the directions of the color shifts leading to whiteness and tint perception are CCT-independent. A similar study was performed in [21] with comparable results.

In an earlier study [22], participants observed white samples under an source with a color filter and were asked if the filter enhanced or reduced perceived whiteness. For a variety of sources with CCTs ranging from 2800K to 7000K, whiteness was enhanced with a blue filter and reduced with green and yellow filters. The trends were comparable at all CCTs studied.

Besides, it was reported in [13] that human ranking of a set of white papers in an indoor office environment correlated well with colorimetry measurements performed under a quartz-tungsten-halogen source (CCT \approx 3000K).

Therefore, experimental data suggest that the color shifts influencing whiteness are similar under a wide range of CCTs. This result is fortunate: it implies that, while Eq. (2) defines whiteness under a 6500 K source, objects designed for enhanced whiteness may retain this property at other CCTs – provided the source allows excitation of FWAs.

2.3. Whiteness formula for other CCTs

As discussed in Section 1, it would be desirable to quantify whiteness under any CCT – either to compare the relative whiteness of objects under a source, or the relative whiteness of an object under various sources. Several approaches can be considered.

One approach is to employ chromatic adaptation: the coordinates of samples under a given source are transformed into D65 illumination, and Eq. (2) is applied. Unfortunately, this does not seem to yield sensible results: as shown in [21], the color coordinates of various white objects fall way out of the bounds of application of Eq. (2) after adaptation. For instance, when the initial source has a CCT \approx 3000 K, all whiteness values obtained by this procedure are negative – an unsatisfactory and incorrect result, since the corresponding objects are actually perceived as white. This failure is likely due to an imperfection in the formulation of the color transformation and the color spaces, together with Eq. (2)'s high sensitivity to color coordinates.

We propose as an alternative to adapt Eq. (2) to the source of interest. This approach is supported by our discussion in 2.2 – namely, the same color shifts have a similar effect on whiteness across a wide range of CCTs. The quantities defining Eq. (2) can be adapted as follows: (x_0, y_0) are now the coordinates of the new reference source; η is recomputed accordingly; ω and φ are assumed to be unchanged for a different CCT. This last assumption is motivated by our previous discussion and the lack of additional data for warm-white sources; further perception studies would be required to establish accurate values. Nevertheless, we do not expect that these refinements would substantively influence relative whiteness rankings. [23]

Figure 2 illustrates the geometry used in generalizing the whiteness equation.

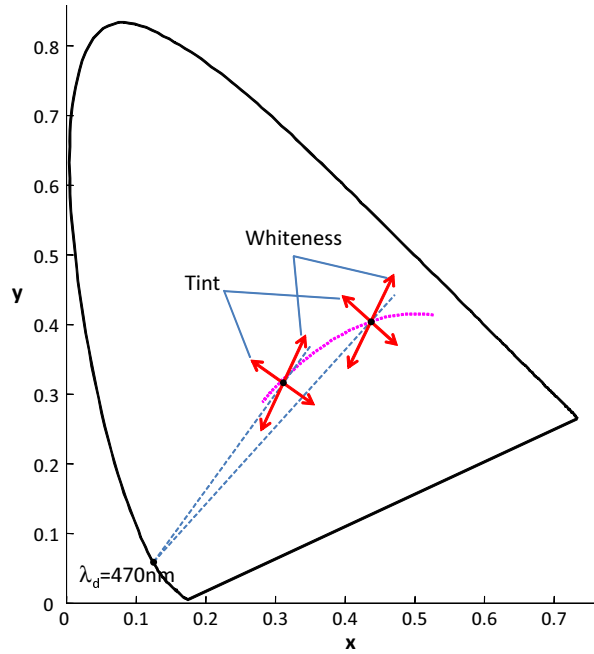


Fig. 2. Geometry for the generalization of the whiteness formula. For any source, the same construction can be applied as for D65, by considering color shifts parallel and perpendicular to the $\lambda_d = 470$ nm direction. Here this is illustrated for two sources on the blackbody locus (dotted line) at 6500 K and 3000 K.

As an example, we propose adaptation to a 3000 K source on the blackbody locus using the 2° CMFs. This yields $(x_0, y_0) = (0.4370, 0.4041)$, $(x_d, y_d) = (0.1241, 0.0578)$, $\eta = 47.9^\circ$ and:

$$W = Y + 810(x_0 - x) + 1700(y_0 - y) \quad (5)$$

The numerical values of Eq. (5) are very similar to those in Eq. (2) after rounding, which is coincidental (the switch from the 10° to the 2° CMFs and the change in CCT from 6500 K to 3000 K have compensating effects on the numerical values, as shown in Appendix A).

Likewise, we propose a modification of the tint equation at 3000 K as follows (using $\eta' = \eta$, and keeping the value of ζ):

$$T = 820(x_0 - x) - 740(y_0 - y) \quad (6)$$

A value of zero indicates an absence of tint. T is a sensitive metric: a value of a few points indicates an object with a non-white appearance. At 6500 K, the tolerance is $-4 < T < 2$ [16,

18]. This value can be used as a guideline at other CCTs, although additional experimental work would be desirable to accurately establish tolerable limits of tint.

Appendix A provides numerical values of the coefficients in the whiteness and tint formulas for CCTs between 2000 and 7000 K.

3. Applications of the whiteness formula

3.1. Description of samples and sources

As an application example, we consider how various sources render whiteness for a series of nine calibrated whiteness standards provided by Avian Technologies (FTS series, matte). The CIE whiteness of the samples, measured by the samples provider, varies between 83 and 140 (outdoors whiteness, *i.e.* D65 illumination). The sample with the lowest whiteness contains no FWA, while the other samples contain an increasing amount of FWA. The FWA employed in these samples is chosen to closely mimic the typical behavior of a whitened commercial paper. We label these samples as W_{xx} , where xx is the CIE whiteness.

The light sources we consider have a CCT of 3000 K. They are a blackbody (BB) radiator representative of an incandescent source; a typical blue-pumped 2-phosphor white-emitting LED (BLED) with a color rendering index (CRI) ≈ 80 ; and a series of six violet-pumped 3-phosphor white-emitting LEDs (VLEDs) with varying violet contribution in the spectrum.

Interest in violet-pumped LED systems is motivated by recent demonstrations of very high performance VLEDs [24] and white sources based on these LEDs. It is expected that the violet content in these sources should be able to excite FWAs and contribute to whiteness. The series of spectra we consider have a violet leak (e.g. fraction of the spectrum below 430 nm) varying between 1% and 10%, and are color-balanced to be on the blackbody locus at 3000 K. These spectra all display excellent CRI (between 90 for the lowest violet leak and 97 for the high violet leak values) and deep-red rendering R9 (also in the range 90-95). We label the VLED with $x\%$ violet leak as a $x\%$ -VLED.

The BLED spectrum was chosen as representative of commercially available MR-16 lamps. Although its CRI is lower than that of the VLEDs, this is not expected to influence whiteness results because the CRI difference is due to the absence/presence of deep red content in the spectrum, a fact irrelevant to the fluorescence of FWA-containing objects.

3.2. Optical characterization procedure

In order to compute the color coordinates of a sample under a given source, we first characterize its (spectral) reflectance and (bispectral) luminescence properties. We employ the double-monochromator method (described in details in [25, 26] and employed in a similar context in [11]) which we shortly summarize below.

In general, if a sample is illuminated with a beam of wavelength λ and unit intensity, the total light leaving the sample (or total spectral radiance) can be written as $E(\lambda, \lambda') = R(\lambda) + L(\lambda, \lambda')$, where R is the reflectance and L the luminescence (due to FWAs in our case). If we measure E for a variety of λ , we obtain the 2-dimensional matrix $E(\lambda, \lambda')$ of the sample's optical response. In other words, the sample's response spectrum under a source of spectrum S is $E \cdot S$, where S is a column vector. The reflectance R is the diagonal of E . We note that R and L are also called the spectral reflected and bispectral luminescent radiance factors [25].

In practice, E is measured as follows. We use an integrating sphere connected to a spectrometer with a CCD-array detector. The relative response of the system versus wavelength has been calibrated. The sample is placed at the output port of the sphere. A collimated monochromatic beam at wavelength λ enters the sphere through a small port, and can be displaced laterally to hit the sample or the wall of the sphere. The beam is first directed to the wall, and the reference spectrum I_0 is collected (this signal is peaked around λ , with a total width of ± 3 nm).

The beam is then directed to the sample, and the resulting spectrum I is collected; we then have $E(\lambda') = I/I_0$. The part of E which is within ± 3 nm of λ is identified as R , while the rest of E (if present) is attributed to luminescence and constitutes L . By repeating the procedure for multiple values of λ , we obtain the full matrix $E(\lambda, \lambda')$. The total procedure takes a few minutes. Our procedure assumes that R and L have the same angular dependence – a safe assumption for the present matte samples (see Appendix B for further discussion). For illustration, Fig. 3 displays the reflectance $R(\lambda)$ and luminescence $L(380, \lambda')$ spectra for samples W115 and W130.

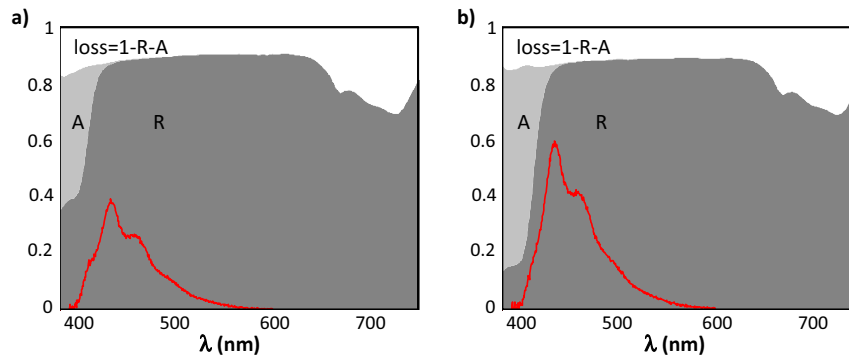


Fig. 3. Optical properties of a) W115 and b) W130. The shaded areas depict reflectance/luminescence as a function of excitation wavelength λ . Deep gray: reflectance (R); light gray: FWA absorption (A) e.g. fraction of the light which is absorbed and re-emitted as luminescence L ; white: loss. The superimposed red line is the luminescence spectrum $L(380, \lambda')$ at an excitation wavelength $\lambda = 380$ nm (amplitude in arbitrary units).

Using this procedure, we characterize each whiteness standard. The various source spectra are then employed to compute the output spectra of the sample. From these we derive the chromaticity coordinates (x, y) and apply Eq. (5). As an example of this procedure, Fig. 4 displays the computed output spectra of the W130 sample under several sources.

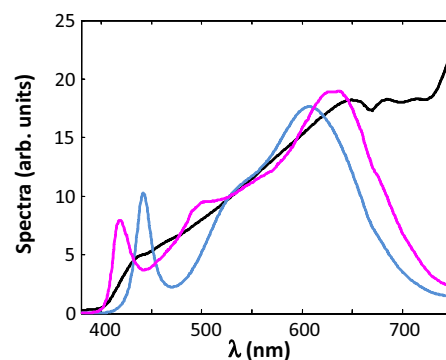


Fig. 4. Computed output spectra of the W130 sample illuminated by a BB radiator (black), a BLED (blue) and a 6%-VLED (magenta).

In order to confirm the accuracy of our characterization procedure, we also compare its predictions with direct measurements under illumination by various lamps. The results, presented in appendix B, show excellent agreement.

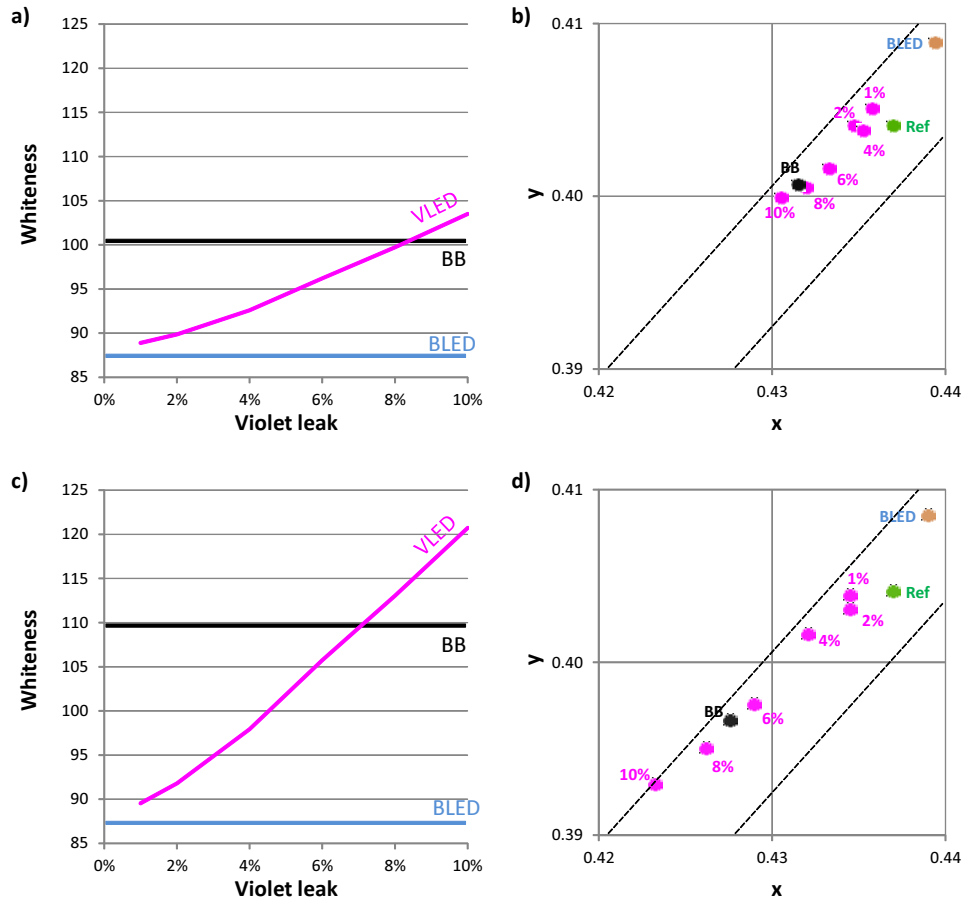


Fig. 5. Whiteness of two objects under various sources. (a) W115 sample: whiteness under illumination by VLEDs, versus violet leak (magenta line). The horizontal lines are the whiteness under illumination by a BLED and a 3000 K BB radiator, respectively. (b) Corresponding (x, y) coordinates. The points correspond to the reference white point of the sources ("Ref"), the BLED, the BB radiator and the VLEDs, (label = violet leak value). The dashed lines correspond to tint values of ± 3 . (c-d) Same as (a-b) for the W130 sample.

3.3. Results

Application of Eq. (5) to the computed spectra yields the whiteness values shown on Fig. 5, for samples W115 and W130. For both samples, the UV tail of the blackbody source induces fluorescence and increased whiteness. As expected, the VLEDs display increased whiteness with increased violet leak. The BLED consistently displays a low whiteness (slightly worse than the 1%-VLED and much worse than the BB radiator). This is expected, as the absence of any violet component in the spectrum of a BLED will fail to excite the FWAs.

The whiteness variations on Fig. 5 are substantial: they span 20 to 30 points. As discussed in Section 2.1, this corresponds to a significant change in the whiteness perception (equivalent to 20-30 points of luminance factor). Overall, the whiteness induced by a BB is well matched by VLEDs with 6-8% violet leak. On the other hand, BLEDs don't induce enhanced whiteness; the value of ≈ 85 obtained for both samples corresponds to a distinctly yellow perception.

Equally informative are the color coordinates of the objects plotted in Fig. 5b and 5d. There is a substantial color shift depending on the source, which is aligned with the direction of whiteness enhancement. Sources with little UV/V content, such as the BLED, sit in the upper-right quadrant of the plot, beyond the reference white point: these samples display decreased whiteness ($W < 100$) despite the presence of FWAs.

We also note that both standards show a slight green tint (about 1-2 points) – this is a property of the objects. None of the light sources cause a significant additional tint effect.

Figure 6 shows the resulting whiteness for the full series of standards, as a function of their CIE (D65) whiteness, for three sources (the BB, the BLED and the 8%-VLED). Our proposed measure of whiteness is well correlated with CIE whiteness for the BB and VLED (however, the whiteness values at 3000 K are slightly lower than the CIE whiteness, which is due to the very high UV/V content of D65). The whiteness values under these two sources are quite close across the whole sample set. For the BLED, on the other hand, no fluorescence is induced; the slight whiteness variations are due to small changes in the samples' reflectance spectra.

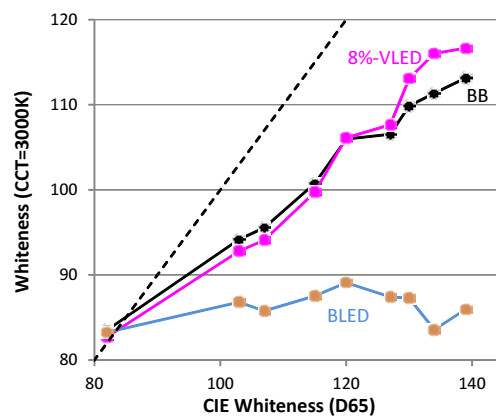


Fig. 6. Whiteness of 3000 K sources versus CIE whiteness, for the series of whiteness standards. The BB and VLED show similar behavior and their whiteness increases with CIE whiteness, as expected. The BLED, however, shows no trend due to a lack of fluorescence. The dashed line shows the diagonal $x = y$: all 3000 K sources induce less whiteness than D65. For W82, which contains no FWAs, all sources yield the same whiteness.

To further illustrate the difference in the sources' behavior, we compute the color distance $D_{uv} = 1000\sqrt{\Delta u^2 + \Delta v^2}$ between a sample illuminated by the blackbody emitter and the various LED sources. This is relevant in a situation where one wishes to retrofit a halogen source with an LED source, and color matching to the halogen is sought. Figure 7 shows the results for several sources and the series of white standards. The BLED induces a large color distance which increases with CIE whiteness. It is above 2 points (a just-noticeable difference) for all fluorescent samples, and reaches 6-8 points for a CIE whiteness of 130-140, typical of many whitened materials. The 4%-VLED shows a reduced D_{uv} , and the 6%-VLED displays a non-noticeable D_{uv} (below 1 point for all samples). Again, a violet leak in the range 6–8% appears optimal to mimic the whiteness generated by a halogen source.

Besides the nine whiteness standards presented here, measurements were also performed on several commercially available papers (including printing papers and a business card paper). Such paper samples typically have a CIE whiteness in the range 120-150. The results obtained on these samples were fully consistent with those obtained on the high-whiteness standards, indicating that our conclusions apply to real-world materials.

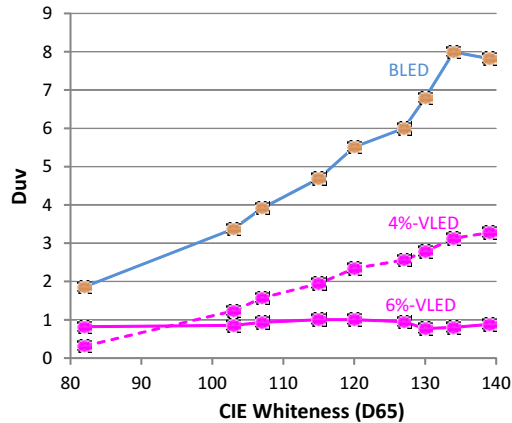


Fig. 7. Color distance D_{uv} between a halogen source and various LED sources, for the series of white standards. $D_{uv} = 2$ corresponds to a just-noticeable difference. The BLED causes large color shifts for whitened objects, while the 6% VLED shows a minimal D_{uv} .

3.4. Discussion

Our application of the adapted whiteness formula indicates significant changes in whiteness depending on the light source, which are expected to be readily perceived by an observer. One can therefore wonder if this is indeed validated by human experience.

A preliminary study was performed, with fifteen participants. Each participant observed two side-by-side unlabeled display booths containing a sheet of commercial white paper, illuminated respectively by a 4%-VLED and a 6%-VLED. The booths were painted with a high-reflectivity white paint and a calibrated Munsell N8 paint, yielding spectrally flat booths. The LED sources were carefully selected to have a very similar white point, so that the participants could not notice a chromatic difference in the empty booths lit by the various lamps. The participants, who had no knowledge of the research question, were asked to compare the whiteness of the paper in the two booths and to express one of five choices: a moderate or strong preference for either booth, or no preference. Two subjects indicated a moderate preference for the 4%-VLED, while the thirteen others preferred the 6%-VLED either moderately (ten subjects) or strongly (three subjects). This is a rather pronounced signal in favor of the higher violet leak, especially considering the moderate 2% difference in violet leak for this pair.

Further, one of the present authors (AD) tried ranking the nine (unlabeled) whiteness standards visually under various sources. A good agreement with the CIE whiteness rank was achieved with a 6%-VLED (with a few inversions of nearest-neighbor samples). When watching side-by-side two samples with a 20-point difference in whiteness under the 6%-VLED, a difference was readily perceived. Under BLED illumination, on the other hand, the sample ranking was impossible and all samples appeared yellowish.

These observations are qualitatively compatible with the numerical results presented above. A proper confirmation of these observations would require a controlled human perception study. Besides, more quantitative assessment is desirable – for instance, the value of the scaling factor ω and tint tolerance should be assessed experimentally, again calling for psychophysical studies. Such studies are currently being finalized in order to test and refine our proposal, and will be the object of future publications.

4. Conclusions

Whiteness enhancement by FWAs is routinely used in a variety of manufactured materials. This effect is well captured by the CIE whiteness formula; however this formula employs a 6500 K illuminant and does not apply to other CCTs. Yet many of these materials are designed to be observed under a variety of lighting conditions, including indoors situations where warmer CCT light sources are common. It is desirable to have a method to quantify whiteness in these situations, including changes in whiteness that result from illumination.

We have proposed a generalization of the CIE whiteness formula to sources of other CCTs. This generalization appears reasonable in view of the geometric foundations of the whiteness formula, and of past human factor studies which suggest that similar color shifts induce enhanced whiteness at various CCTs.

As an application of our formula, we have shown how various 3000 K sources are able to harness enhanced whiteness on fluorescent objects. Incandescent sources induce significant whiteness due to their UV/V content. Typical blue-pumped LED sources, on the other hand, show no whiteness enhancement due to the absence of short-wavelength radiation in their spectra. Violet-pumped LEDs offer an attractive alternative: by tuning the amount of violet light in the spectrum, enhanced whiteness can be restored – at no expense on other color-quality metrics such as CRI and R9, which can be maintained to values beyond 95.

We have also exemplified the impact of FWAs in terms of color difference to a halogen source. In retrofit applications, a good color match is essential – hence the use of color rendition metrics such as the CRI. However, we conclude that even a blue-pumped LED with a decent CRI (≈ 80) can cause a significant perceptual difference for FWA-containing objects. Since this issue is due to a lack of violet radiation, it would not be solved by blue-pumped LEDs with a very high CRI.

Considering the importance of white perception in the pleasantness of objects' appearance, such effects are important for adoption of LED sources for general illumination. We suggest that a source's ability to render and enhance whiteness should be considered as a key metric for the quality of light, together with metrics that quantify color rendition. The use of our proposed formula together with standardized whiteness samples, as presented here, constitutes one possible approach. Human factor studies, necessary to confirm our results, are underway and will be the object of future publications.

A. Numerical values of the whiteness and tint equations vs. CCT

In general, Eq. (2) can be expressed as:

$$W = Y - P \cdot (x - x_0) - Q \cdot (y - y_0) \quad (7)$$

As explained, the values of P and Q can be derived for any CCT taking into account the chromaticity coordinates of the source. Figure 8 indicates the numerical values of P and Q obtained by this method for sources on the blackbody locus. These coefficients can be employed to generate a whiteness formula for a source of any CCT between 2000 and 7000 K.

B. Verification of the samples' optical characterization procedure

In Section 3.2, we describe how the optical properties of samples with FWAs are characterized. In this Appendix, we check the accuracy of this characterization procedure.

Once the total spectral radiance E of a sample is known, one can compute the optical output S' of the sample illuminated by a given source of spectrum S as $S' = E \cdot S$, and compare this theoretical spectrum to an actual measurement of the sample under illumination.

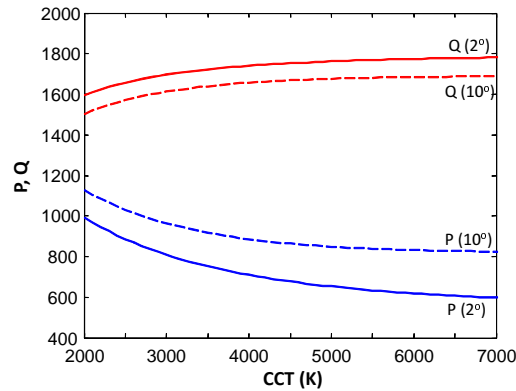


Fig. 8. Values of the constants P and Q in Eq. (7), vs. CCT. The full lines correspond to the 2° CMFs and the dashed lines to the 10° CMFs. The dashed curves at 6500 K have similar values to the full curves at 3000 K – this explains the similar values in Eqs. (2) and (5).

We have selected five MR-16 lamps representative of the sources discussed in this article: an halogen MR-16, a commercial BLED and 3 VLEDs (with violet leakage 3%, 5% and 8%). All have a CCT of 3000K. Each lamp was used to illuminate a white display booth. First, a perfect white diffuser ($R \sim 99 - 100\%$) was placed in the booth and the light diffused by the diffuser was measured by a calibrated imaging spectrophotometer (Photoresearch camera PR650); this gave us access to the emitted spectrum of the source S , which was used to compute S' . Next, we replaced the diffuser by a sample and repeated the measurement to obtain the output spectrum S'' composed of the sample's reflectance and luminescence. By comparing S' and S'' we can assess the accuracy of our measurement of E .

This procedure was performed on the whiteness standards. Figure 9 compares S' and S'' for two standards (W83 and W140) illuminated by each of the five MR-16 lamps. No vertical rescaling was used when comparing S' and S'' . As can be seen, the agreement between S' and S'' is excellent for each of the lamps. Notably, the agreement is extremely good in the violet-blue region where fluorescence occurs, confirming the accurate characterization of the samples' fluorescence properties. The slight differences between S' and S'' correspond to small chromatic shifts: $D_{uv} < 1$ at worst, much less than the chromatic shifts relevant to whiteness enhancement.

The bispectral reflectance measurement uses a 2π diffuse collection ($0^\circ/D$ geometry) while the direct measurement is collected at 45° with a 2° range ($0^\circ/45^\circ$ geometry). The agreement of the two measurements confirms the hypothesis that the sample's reflection and luminescence have the same angular dependence.

Thus we conclude that the two techniques (direct measurement and bispectral reflectance) are in excellent agreement. The advantage of the latter technique is that it can be applied numerically to a variety of spectra (either measured or simulated). This enables, for instance, the evaluation of whiteness for a large set of spectra without requiring lamps to be fabricated. As a side note, this approach can also advantageously be used to compute CIE whiteness with illuminant D65, thus circumventing the difficulty to simulate D65 in a spectrophotometer (a known limitation to the practical estimation of CIE whiteness).

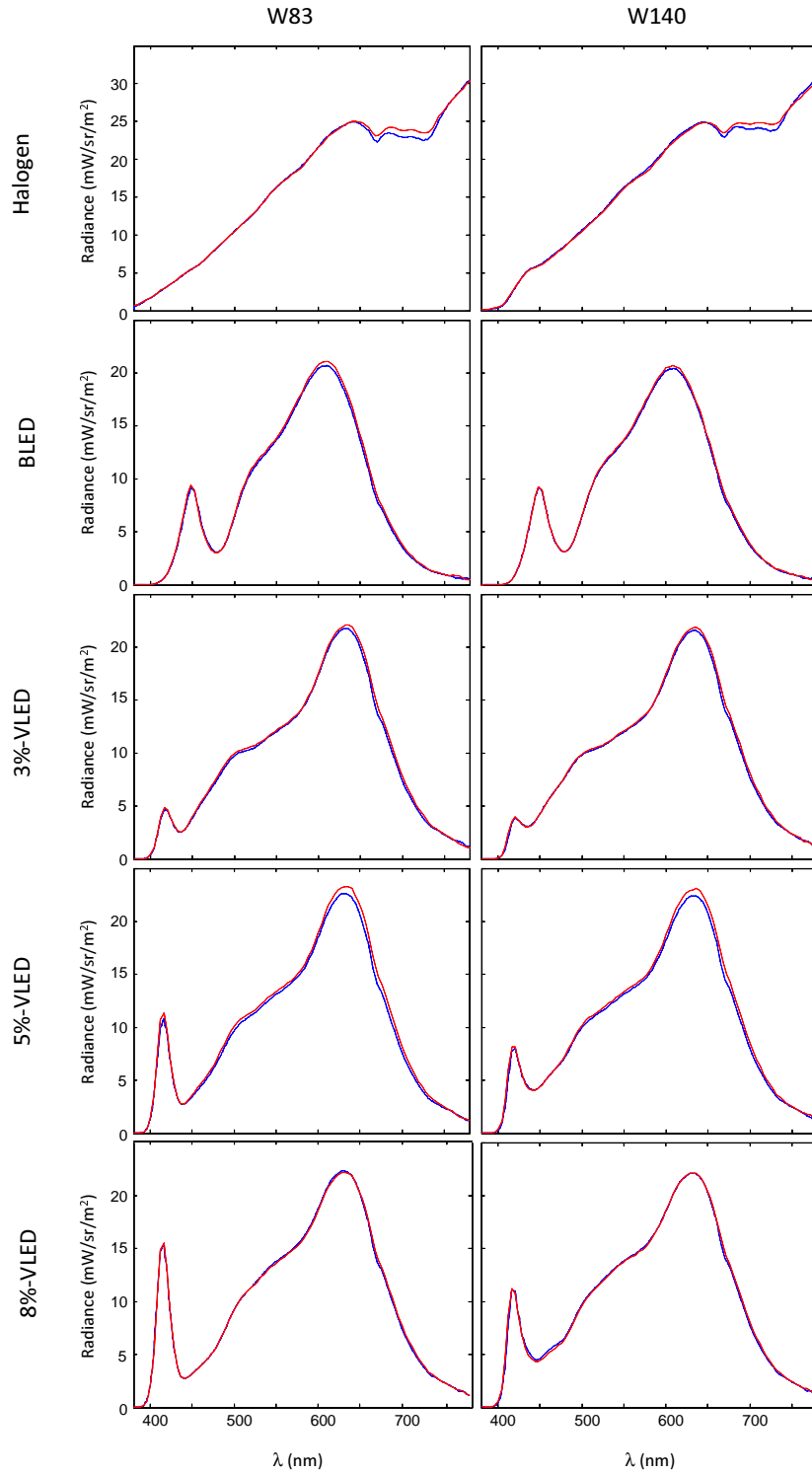


Fig. 9. Comparison of the output spectra derived from bispectral reflectance (blue curves) and directly measured with an imaging spectrophotometer (red curves), for two whiteness standards illuminated by five lamps.